Electric-field dependence of interband transitions in $In_{0.53}Ga_{0.47}As/In_{0.52}Al_{0.48}As$ single quantum wells by room-temperature electrotransmittance

A. Dimoulas, K. P. Giapis,[a] J. Leng,[b] G. Halkias, K. Zekentes, and A. Christou[c]
Foundation for Research and Technology-Hellas, P.O. Box 1527, Heraklion 71110, Crete, Greece

(Received 3 January 1992; accepted for publication 13 May 1992)

Room-temperature electrotransmittance has been used in order to investigate the interband excitonic transitions in a 250-Å-thick $In_{0.53}Ga_{0.47}As/In_{0.52}Al_{0.48}As$ single-quantum-well system as a function of an externally applied electric field. Parity forbidden transitions, involving conduction-band states with quantum numbers up to $n=5$, which become more pronounced at high electric fields were observed. The ground-state and the forbidden transitions showed a significant red shift due to the quantum confined Stark effect. A comparison with previously reported results on thinner InGaAs/InAlAs quantum wells indicated that the wide-well sample exhibits the largest shift, as expected from theory. Despite the appreciable Stark shift, the rather large, field-induced linewidth broadening and the relatively low electric field at which the ground-state exciton is ionized poses limitations on using this wide-quantum-well system for electro-optic applications.

I. INTRODUCTION

Quantum-well (QW) structures of $In_{0.53}Ga_{0.47}As$ with $In_{0.52}Al_{0.48}As$ barriers have attracted interest because of their applications in optoelectronic devices. The recent observation[1] of second-harmonic generation due to intersubband transitions in coupled InGaAs/InAlAs QWs shows potential for using this system in far-infrared detectors at $\lambda \simeq 10$ μm. In addition, because of the small band gap of $In_{0.53}Ga_{0.47}As$, optical devices based on the above QW system can operate at long wavelengths (1.55 μm) suitable for optical fiber communication applications.[2] A class of optoelectronic devices of current interest includes optical modulators[3] and self-electro-optic-effect devices,[4] used as components for optical signal processing and optical logic. Both kinds of devices utilize multiple quantum wells (MQW) and take advantage of the quantum confined Stark effect (QCSE).[5] According to this effect, a shift in energy position of the excitonic absorption resonances results when an electric field is applied perpendicular to the confinement plane. The GaAs/AlGaAs QW system under high electric fields has been extensively studied during the last decade.[6] Considerably less amount of work has been devoted to the investigation of $In_xGa_{1-x}As$ QWs. The dependence of interband transition energies on the electric field in the pseudomorphic $In_xGa_{1-x}As/GaAs$[7] and $In_xGa_{1-x}As/AlGaAs$[8] QW systems has been studied by photocurrent and electroreflectance spectroscopy. Asymmetric coupled $In_{0.53}Ga_{0.47}As/In_{0.52}Al_{0.48}As$ QWs,[9] studied by electroabsorption, indicated large shifts with applied electric fields due to resonant coupling of electron subbands. Appreciable red shifts due to the QCSE were measured by photocurrent at 300 K in *p-i-n* modulator structures, utilizing 105-Å-thick $In_{0.53}Ga_{0.47}As/In_{0.52}Al_{0.48}As$ MQWs.[10] A similar behavior was observed in 103 Å MQW structures of the same material system probed by Schottky barrier electroabsorption at 2 K.[11] It is predicted theoretically that wider quantum wells exhibit larger Stark shifts but this has not yet been reported experimentally for the InGaAs/InAlAs QW system. Wide QWs are also interesting from the standpoint of physics, since they permit observation of higher conduction- and valence-band states and can facilitate the study of fundamental optical properties of quantum confined structures.

In the present work, we have investigated $In_{0.53}Ga_{0.47}As/In_{0.52}Al_{0.48}As$ single QWs with a well width of 250 Å by using electrotransmittance (ET) at room temperature. A large number of parity allowed interband transitions is observed, which lose oscillator strength to forbidden transitions with increasing electric fields. Large Stark shifts were measured for the lowest allowed and higher forbidden interband transitions and compared with previous theoretical and experimental results for thinner quantum wells. We have also studied the broadening of the ground-state transition as a function of the electric field and found it to be of the same order of magnitude as the shift of the corresponding peak energy position. Our work provides more insight into the factors, which affect the excitonic linewidth and limit the efficiency of electro-optic devices.

II. EXPERIMENTAL DETAILS

The SQW was grown by molecular-beam epitaxy on n^+-InP (001) substrates and it had the following structure: (0.3 μm) $In_{0.52}Al_{0.48}As$/250 Å $In_{0.53}Ga_{0.47}As$/(1.0 μm) $In_{0.52}Al_{0.48}As/n^+$-InP (001). Our optimization studies of the MBE growth of InAlAs have pointed out that the best material, in terms of electrical properties and

[a]Present address: AT&T Bell Laboratories, 600 Mountain Ave., Murray Hill, NJ 07974.
[b]Permanent address: Zhenjiang Shipbuilding Institute, People's Republic of China.
[c]University of Maryland, College of Engineering, College Park, MD 20742.

 0021-8979/92/171912-06$04.00

photoluminescense characteristics is grown at a substrate temperature of 530 °C. However, in this study, both InAlAs and InGaAs layers were grown at the same temperature of 500 °C, which is also compatible with the growth of InGaAs. This was done in order to avoid layer interdiffusion effects and achieve abrupt heterointerfaces. In addition, such an intermediate growth temperature of InAlAs could suppress the tendency for alloy clustering in this material, which influences the quantum-well linewidths, as previously suggested. The growth rate was 0.85 μm/h, while the V/III equivalent beam pressure ratio was 25. Scanning electron microscopy observations indicated that relatively smooth surfaces were obtained with a few hillocks elongated along the [011] direction. The samples were unintentionally doped n type to about 10^{14} cm^{-3}. The quantum well was characterized by photoluminescence at 12 K. The measured full width at half-maximum of 8.5 meV of a single peak centered at 0.815 eV compares favorably to the best reported values[12] and it is indicative of good alloy quality and smooth interfaces.

The electric field was applied through a semitransparent Schottky contact, 500 μm in diameter, which was made by depositing 100 Å of Ti by e-beam evaporation on the top InAlAs layer. The ohmic contact was made on the n^+-InP substrate by using Au/Ge/Ni. The Schottky diode had 10 and 180 nA leakage current at 5 and 15 V reverse bias, respectively. In our experimental arrangement, we have operated the devices under reverse dc bias conditions in the range between 0 and 15 V. A small ac bias, provided by a voltage generator in a square-wave form with a frequency of 300 Hz and peak-to-peak amplitude of 0.25 V, was superimposed on the dc voltage. The ac bias was used to perturb the built-in electric field and modulate the transmittivity of the QW region. The transmitted light was detected by an EG&G InGaAs p-i-n photodiode operating in the photovoltaic mode and the ac part of it, proportional to the transmittivity changes ΔT, was detected by a lock-in amplifier tuned at the modulating frequency. The dc part, proportional to the transmittivity T, was measured by a voltmeter. By using a double grating $\frac{1}{4}$ m SPEX monochromator to analyze incident light, the normalized quantity $\Delta T/T$ was finally obtained as a function of photon energy. The spectral range covered in the electrotransmittance experiments was from 0.7 to 1.35 eV. The lower limit was due to the limited response of the photodiode, while the upper limit was determined by the onset of absorption from the InP substrate. The experimental error in the measurements of the transition energies and broadening parameters was dominated by the resolution of the monochromator limited to 2 nm.

III. DESCRIPTION OF THE ELECTROTRANSMITTANCE SPECTRA

The room-temperature ET spectrum of the 250 Å $In_{0.53}Ga_{0.47}As/In_{0.52}Al_{0.48}As$ QW structure is shown in Fig. 1 for five different values of reverse bias. At zero reverse bias as much as seven optical excitations are clearly resolved. These are attributed to allowed excitonic interband transitions of the type nnh between confined electron and heavy-hole states, having the same principal quantum number n. (The transitions are labelled by using the notation nmh, where n and m are the quantum numbers of the conduction- and valence-band states, respectively, and h denotes the heavy-hole band.) Light-hole-related transitions have not been observed, in accordance with previous reports,[11] for the lattice-matched InGaAs/InAlAs QW system by electromodulation spectroscopy. Due to selection rules, the intensity of the light hole (lh) is about $\frac{1}{3}$ of the intensity of the heavy-hole (hh) transition, so that, in general, lh appears weak in optical spectra as compared to hh. In the InGaAs/InAlAs heterostructure system, alloy disorder in the well and interface roughness[13] result in a broadening of the exciton peaks, which is more severe for the lh (almost by a factor of 2 bigger than that corresponding to the hh[14]). Since lh transition is also weak, the enhanced broadening makes it difficult to resolve and the optical spectra are dominated by the hh excitation.

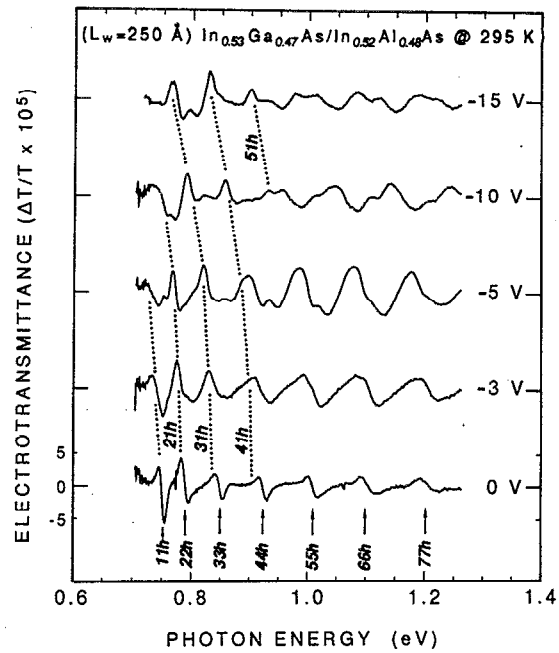

FIG. 1. Electrotransmittance spectra of the 250 Å $In_{0.53}Ga_{0.47}As/In_{0.52}Al_{0.48}As$ quantum well, at 295 K, for five different values of reverse bias. The spectra are displaced with respect to one another by a constant portion, corresponding to the scale shown with the zero-bias spectrum. Arrows mark the allowed interband excitonic transitions, which are clearly resolved in the zero-bias spectrum. The dotted lines trace the energy position of the ground-state and the higher forbidden transitions, which show a red shift of the 1h state due to the QCSE.

The increase of the nnh peak linewidth with the quantum number n, seen in the 0 V spectrum of Fig. 1, is attributed to the effect of interface roughness, as described elsewhere.[15] By increasing the reverse bias V_b, it can be seen that the peaks become broader and shift to lower energies. The increased linewidth may be explained in terms of electric-field-induced shortening of the exciton lifetime. The broadening is more pronounced for the higher transitions, causing an overlapping between adjacent peaks, so that the last three peaks cannot be clearly

resolved for $V_b > 3$ V. The red shift of the peaks may be understood in terms of the QCSE.[5,16] According to this effect, increasing electric field results in downward (upward) movement of the $n=1$ electron (hole) states, so that the spectral position of the ground-state optical transition moves to lower energies. This explains satisfactorily the red shift of the $11h$ transition seen in Fig. 1. However, it is apparent from the same figure that there exist other higher excitations, which also exhibit large red shifts at large reverse biases, as traced by the dotted lines. These cannot be attributed to higher allowed transitions of the type *nnh* because, according to previous theoretical[11,17] and experimental results,[6,7,10] the higher ($n>1$) electron and hole states are insensitive to electric fields. Their behavior can only be explained by assigning them to normally forbidden transitions of the type $n1h$ since the involvement of the $1h$ state is consistent with such large red shifts.[16] Although transitions of the type $1mh$ could behave similarly with the electric field, these have not been considered because their theoretical energy positions lie lower than the experimentally observed peaks.

Parity forbidden transitions under high electric fields have been previously reported by photocurrent (PC) measurements in $GaAs/Al_{0.34}Ga_{0.66}As$ (Ref. 6) and $In_xGa_{1-x}As/GaAs$ (Ref. 7) MQWs at 77 and 2 K, respectively. Photocurrent and electroreflectance at 300 K were used to observe the $12h$ and $21h$ transitions in 100 Å $In_{0.17}Ga_{0.83}As/Al_{0.3}Ga_{0.7}As$ strained MQWs.[8] In $In_{0.53}Ga_{0.47}As$ MQWs with lattice-matched $In_{0.52}Al_{0.48}As$ barriers the $21h$ and $13h$ transitions were resolved by PC[10] and electroabsorption[11] at 300 and 2 K, respectively. In the above mentioned works the forbidden transitions are unresolvable in the low-electric-field spectra, but they gain intensity at higher electric fields, where they can clearly be resolved. The previously assigned peaks $21h$, $31h$, $41h$, $51h$ of Fig. 1 follow a similar behavior. Because of the large well width, in the zero-field spectrum, these peaks are close to the corresponding *nnh* allowed transition energies. At low fields the latter excitations *nnh* are dominant, but as the electric field increases, they lose oscillator strength to the forbidden transitions.[11] These develop as low-energy shoulders to the *nnh* peaks for V_b up to 3 V and become dominant for bias higher than 5 V.

It is apparent from Fig. 1 that, for applied biases $\geqslant 3$ V, the evolution of the higher-order transitions ($n \geqslant 5$) cannot be clearly deconvoluted and traced down. The situation becomes even more complicated with the appearance of several weak peaks, as occurs in the 5 V spectrum, for example. To illustrate the difficulties in assigning these peaks, consider the case of the weak "bump" on the high-energy side of the $41h$ transition in the 5 V spectrum. This is believed to be a result of the overlapping of the $44h$ and $51h$ transitions. These two transitions are well separated in energy in the 0 V spectrum. However, when the reverse bias increases, the spectral position of $44h$ remains unchanged while $51h$ shifts to lower energy, coming closer to $44h$. This partial overlap results in a "ghost" feature in the form of a bump in the 5 V spectrum. At higher reverse bias, the $44h$ transition decreases in intensity and the $51h$ becomes dominant, while its energy position also changes. This behavior results in the disappearance of the bump at higher reverse bias. The above considerations are further supported by the fitting results. Indeed, it was found necessary to consider two transitions close in energy, in order to reproduce the bump by using the fitting model of Sec. IV A. If instead only one transition is considered, it is not sufficient to provide a good fit to the 5 V spectrum at the vicinity of the "ghost" feature.

It is worth mentioning here that ET is a very sensitive technique in observing parity forbidden transitions as opposed to other optical techniques, such as absorption and photocurrent (PC) spectroscopies. Indeed, in PC spectra (not shown here) of the same QW sample, forbidden transitions appear much weaker, while allowed excitations give the dominant contribution even at high electric fields. A similar behavior has been previously observed in the 4 K data of Fritz *et al.*[8] from InGaAs/AlGaAs MQWs. In the latter work, the $21h$ was found to be dominant and the $22h$ extremely weak in electroreflectance, while the relative intensities of the two transitions were completely reversed in the corresponding PC spectra.

The enhanced sensitivity of the ET is attributed to the use of a small ac electric field in order to modulate the transmitivity. Parity forbidden transitions are very sensitive to this modulating electric field because it distorts the envelope wave function and results in a violation of the selection rules. This means that a small modulating field results in large intensity modulation of normally parity forbidden transitions, so that intense peaks appear in ET spectra. In the same manner, the appearance of forbidden transitions in ET spectra, under high dc electric fields, can be understood as a result of the breaking of the selection rules so that optical excitations between any of the states in the conduction and valence bands become possible.[6]

IV. ELECTRIC-FIELD DEPENDENCE OF THE TRANSITION ENERGIES AND LINEWIDTHS

A. Electrotransmittance line shapes

Electromodulation spectra exhibit complex line shapes due to their derivative nature.[18] The mixing of allowed and forbidden transitions at high fields adds to the complexity, so that transition energies and linewidths cannot be obtained directly from the spectra by a simple inspection. A fitting procedure is required to determine the above quantities as adjustable parameters. The model used for the fitting assumes that the normalized change $\Delta T/T$ in the transmittance can be expressed in terms of the first derivatives[18] of the absorption coefficient α with respect to the transition energy E_{nmh}, the broadening parameter Γ, and the intensity I of the excitonic transition,

$$\Delta T/T \simeq -L\Delta\alpha, \tag{1}$$

$$\Delta\alpha = \frac{\partial\alpha}{\partial E_{nmh}}\Delta E_{nmh} + \frac{\partial\alpha}{\partial\Gamma}\Delta\Gamma + \frac{\partial\alpha}{\partial I}\Delta I. \tag{2}$$

Here, L is the modulation depth, which is equal to the width of the depletion region. Following our previous

work,[15] for the zero-electric-field spectrum, an inhomogeneously broadened absorption with a Gaussian[18,19] profile α_G can be used as the most appropriate to describe disorder effects introduced by exciton-LO phonon coupling[20] and interface roughness.[15,21] At nonzero electric fields, the absorption is also homogeneously broadened, following a Lorentzian line shape α_L due to field-induced tunneling effects. The resultant absorption profile can be expressed as a convolution of a Lorentzian with a Gaussian function (the Voigt profile).[22] In the present work we have used an approximation to the Voigt profile by taking a linear superposition of a Lorentzian and a Gaussian, following the work of Theis *et al.*[23] in fitting their GaAs/AlGaAs MQW photoreflectance spectra,

$$\alpha \simeq r\alpha_L + (1-r)\alpha_G. \tag{3}$$

Here, r is the fraction with which the Lorentzian α_L contributes to the functional form of the absorption coefficient α. The experimental values of r, I, Γ, and E_{nmh} were obtained from the best fit to the experimental curves of Fig. 1, according to Eqs. (1)–(3).

This fitting procedure made it possible to distinguish between allowed and forbidden transitions and to follow their peak energy, linewidth, and relative intensity changes with electric field, a task that would otherwise be difficult due to peak overlapping. The fitting was particularly useful in studying the variation with the electric field of the higher allowed transitions whose intensity becomes very weak at high electric fields. The electric-field dependence of the transition energies E_{nmh} and the half-width at half-maximum (HWHM), denoted in the following by Γ, is discussed in subsections B and C, respectively.

B. Dependence of the transition energies on the electric field

The dependence of allowed and forbidden transition energies on the externally applied electric fields is shown in Fig. 2. The electric field can be estimated from the applied external bias in the abrupt junction approximation. However, for a more accurate determination we have employed a charge control variational model[24,25] in which the Schrödinger and Poisson equations are solved self-consistently to provide the band potential profile. This is used to calculate the field at 0.3 μm from the surface, close to the QW region. By setting the surface built-in potential equal to 0.6 V and the doping concentration equal to 10^{14} cm^{-3}, a value of F=4.2 kV/cm was obtained at zero bias, corresponding to the built-in electric field. At the highest reverse bias of 15 V attained in this work, the electric field was F=117 kV/cm. We present here only the transitions up to n=4, since these are the best resolved ones. It can be noted that the higher allowed excitations nnh with $n>1$, are almost independent of the electric field. The 33h and 44h transitions show only a slight red shift at fields higher than 35 kV/cm, while there is an indication of a small blue shift for the 22h excitation above 30 kV/cm. This behavior of the 22h transition has been previously observed in 105 Å InGaAs/InAlAs QWs by Nojima *et al.*[10] and is predicted by theory[17] for all of the higher allowed excitations. For

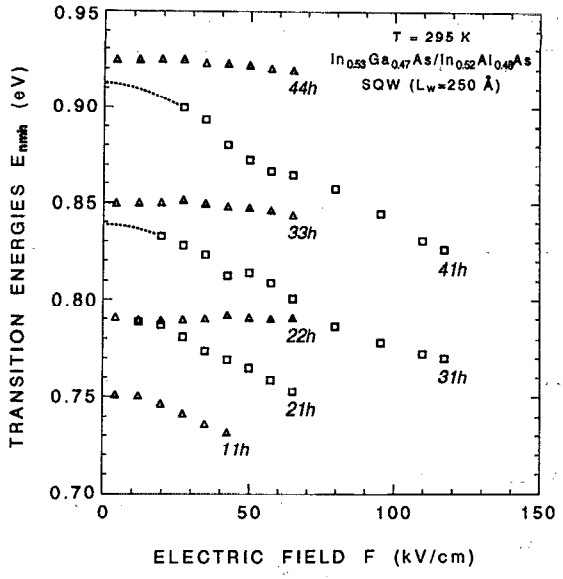

FIG. 2. The dependence of the interband transition energies on the electric field. The higher allowed transitions 22h, 33h, 44h (△) show only a slight variation with the electric field. The 11h (△) and the 21h, 31h, and 41h excitations (□) produce an appreciable red shift due to the QCSE. Dotted lines represent an extrapolation of the 31h and 41h transitions to low electric fields. The experimental error, about 2.0 meV, is too small in the energy scale shown here.

fields higher than 65 kV/cm (V_b = 8 V), there are no data available for all of the nnh ($n>1$) since these transitions become wery weak and cannot be clearly resolved by using the fitting procedure of Sec. IV A. The 11h transition shows a pronounced red shift, due to the QCSE, which is as large as −20 meV for F=45 kV/cm (V_b = 5 V). Above that value the intensity is very weak, due to field-induced exciton ionization. We note here that the exciton binding energy has not been considered in the interpretation and evaluation of the red shift because it is rather insensitive to electric fields. Indeed, according to previous work on InGaAs/InAlAs,[14] in a 100 Å QW, the binding-energy variation is only 0.5 meV at a field of about 120 kV/cm. The dominant contribution to the shift of the transition energies comes from the variation of the free-electron and hole energy states with the electric field.

The forbidden transitions 21h, 31h, 41h, represented by rectangles in Fig. 2, also show a red shift, which is of about the same magnitude as the one of the ground-state transition. This is attributed to the QCSE of the 1h valence band, since the higher-conduction-band states are insensitive to electric fields as has already been explained in Sec. III. Since the intensity of the latter two transitions is very weak at small reverse bias, data are not available for values of F less than 20 kV/cm. However, by making an extrapolation based on the F^2 dependence of the shift at low fields,[26] as shown by the dashed line in Fig. 2, we obtained low-electric-field values for the forbidden transition energies $n1h$ up to n=4. These are listed in Table I, along with the corresponding allowed ones nnh, determined from the fitting of the V_b = 0 spectrum, shown in Fig. 1. In the same table, theoretical values of the transition energies can be

TABLE I. Experimental (expt.) and theoretical (theor.) values of the transition energies for zero electric field. The experimental values for the *nnh* transitions were deduced from the fitting of the zero-field spectrum while the $21h$, $31h$, and $41h$ were determined by using an extrapolation to low fields as shown in Fig. 2. The theoretical values have been calculated by using a finite square-well potential model. All values are expressed in eV.

E_{11h}	E_{22h}	E_{33h}	E_{44h}	E_{55h}	E_{66h}	E_{77h}	E_{21h}	E_{31h}	E_{41h}
				Experimental					
0.751	0.789	0.848	0.924	1.009	1.1	1.204	0.789	0.838	0.912
				Theoretical					
0.756	0.792	0.851	0.933	1.038	1.155	1.301	0.788	0.840	0.914

found, which were calculated by using a finite square-well potential model[27] within the effective mass approximation. The parameters used, were the following:[15] $\Delta E_c = 0.5$ eV for the conduction-band discontinuity; $E_g = 0.745$ eV for the band-gap energy of $In_{0.53}Ga_{0.47}As$; and $m_e^* = 0.041m_e$, $m_h^* = 0.377m_e$ for the effective masses in the conduction and valence band, respectively. The exciton binding energy has not been included in the calculation of the transition energies in Table I. According to previous theoretical work,[14] for a 200 Å InGaAs/InAlAs QW, the heavy-hole-related exciton binding energy is $E_b \simeq 4.2$ meV, while by extrapolating the results to larger well widths it can be inferred that for a 250 Å QW, E_b is less than 3.4 meV. This value, bordering the limits of our spectrometer resolution, is also very small compared to free-electron and hole energies as well as the band-gap energy. Therefore, excluding the exciton binding energy from our calculations does not significantly alter the conclusions from the comparison of experiment with theory in Table I. Indeed, the agreement between theoretical and experimental values of the $21h$, $31h$, and $41h$ transitions is remarkable.

The Stark shifts ΔE_{nmh} obtained in our work for the 250 Å quantum wells are compared, in Fig. 3, with previously reported experimental and theoretical results on the $11h$ transition of thinner $In_{0.53}Ga_{0.47}As/In_{0.52}Al_{0.48}As$ QWs. The shift of the $11h$ transition denoted by full circles in Fig. 3 is only slightly larger than the shift of the $21h$, $31h$, and $41h$ transitions. This is an indication that the ground conduction-band state with $n=1$ has only a small variation with F, while the main contribution to the shift of the $11h$ transition comes from the $1h$ valence-band state.[16] Theoretical curves, reproduced from the work of Bastard and Ferreira,[28] are added in Fig. 3 as solid lines for two different well widths of 150 and 200 Å. Due to the larger well width,[26] the $11h$ Stark shift obtained in the present work is clearly larger than the one predicted for a 150 Å QW as expected, but slightly smaller than the theoretical curve for a 200 Å QW. A comparison with previously reported experimental data in Fig. 3 shows that, for a given electric field, our 250 Å QW gives a considerably larger shift than the one obtained from the $\simeq$103 Å QW of Satzke *et al.*[11] and the 105 and 72 Å QWs of Nojima *et al.*[10] It has to be noticed, however, that the $11h$ transition in the thinner QWs persists at high electric fields, in excess of 150 kV/cm, in contrast with the $11h$ transition of our wide QW

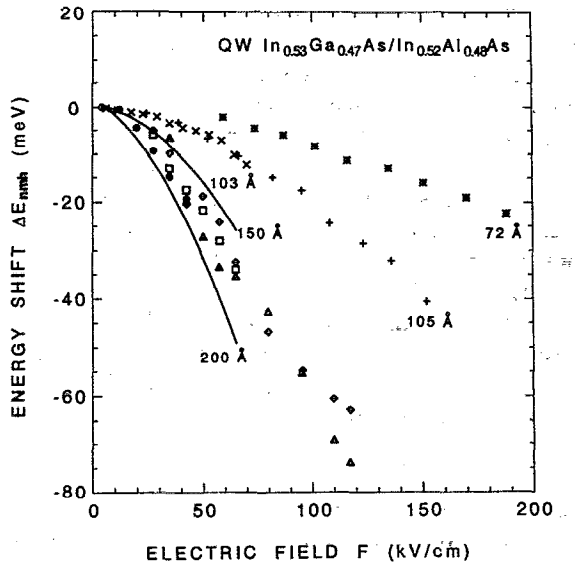

FIG. 3. The Stark shift of several $In_{0.53}Ga_{0.47}As/In_{0.52}Al_{0.48}As$ quantum wells with different well widths. Results from our 250 Å quantum well are represented by (●): $11h$; (□): $21h$; (◇): $31h$; (▲): $41h$. Experimental points for 105 and 72 Å quantum wells, denoted by + and *, respectively, have been reproduced from data of Ref. 10. Experimental data for a 103 Å quantum well taken from Ref. 11 are indicated by ×. Solid lines represent theoretical predictions for 150 and 200 Å quantum wells, reproduced from Ref. 28. The error of our measurements is 2.0 meV.

which becomes very weak for fields higher than 45 kV/cm. At that field, the maximum obtained value for the Stark shift is $\Delta E_{11h} = -20$ meV as seen in Fig. 3. The higher transitions $31h$ and $41h$ of the 250 Å QW, which persist at higher electric fields (>100 kV/cm), produce a shift of about -75 meV, the largest obtained from an InGaAs/InAlAs quantum-well system.

C. Linewidth dependence on the electric field

Electromodulation spectroscopy has an advantage over other optical techniques, such as absorption or photocurrent, in that it is free of background effects, thus enabling a more systematic study of the linewidth as a function of the electric field. This is performed by determining the HWHM Γ_{11h} for the ground-state transition $11h$, based on the fitting procedure of Sec. IV A. The variation of Γ_{11h} with the electric field is plotted in Fig. 4. The linewidth increases from 6 meV at low electric fields up to a value of 20 meV at $F=45$ kV/cm, before the exciton becomes completely ionized. A quantity of interest may be the ratio $\rho = -\Delta\Gamma_{11h}(F)/\Delta E_{11h}(F)$ of the field-induced changes $\Delta\Gamma_{11h}(F) = \Gamma_{11h}(F) - \Gamma_{11h}(0)$ of the HWHM divided by the absolute value of the energy shift of the peak. This ratio ρ as a function of the electric field is also given in Fig. 4. It is seen that the ratio remains almost constant with the field at a value $\rho \simeq 0.8$, indicating that the field-induced change of the linewidth is of the same order of magnitude, although slightly smaller than the Stark shift. In order to achieve high-contrast ratios in optical modulator devices, it is required that the excitonic peaks remain sharp as they shift to lower-energy positions with increasing applied bias

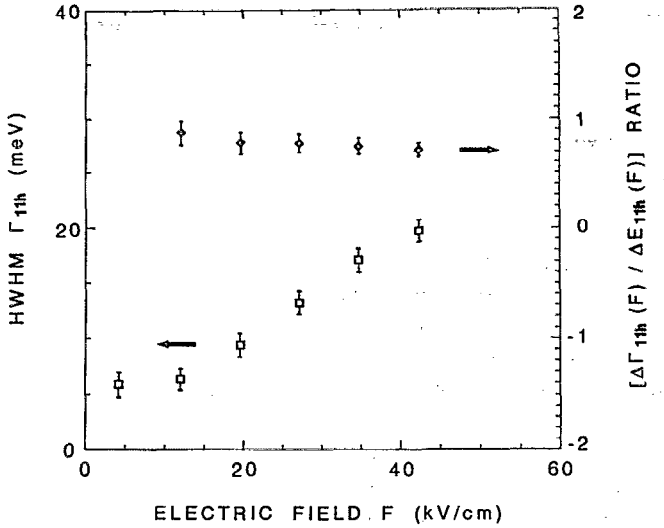

FIG. 4. The dependence of the HWHM of the ground-state transition $11h$ on the electric field is shown on the left-hand-side axis. On the right-hand side axis, the ratio of the field-induced change of the linewidth for the $11h$ transition divided by its corresponding Stark shift is given as a function of the electric field.

($\rho \ll 1$). An electric-field-induced broadening comparable to the peak shift ($\rho \simeq 1$) may result in low-efficiency modulation operation and this is a drawback for the design and fabrication of high-performance electro-optic devices.

V. CONCLUSIONS

In the present work we have used electrotransmittance spectroscopy at room temperature in order to investigate the interband optical transitions of a 250 Å $In_{0.53}Ga_{0.47}As/In_{0.52}Al_{0.48}As$ single-quantum-well structure, under externally applied electric fields. At low electric fields, as much as seven parity allowed interband transitions between states with the same quantum number n were clearly resolved. With increasing electric field, they lose oscillator strength to forbidden transitions of type $n1h$ between the valence-band ground state $1h$ and the higher conduction-band states with $n > 1$. Due to the quantum confined Stark effect, the latter transitions shift rapidly to lower energies by an amount comparable to the ground-state excitation $11h$. In contrast, the higher allowed transition energies were found to be insensitive to the applied field, in agreement with theoretical predictions. A comparison with previous experimental results on thinner quantum-well structures pointed out that, for a given electric field, the largest Stark shift was obtained in our wide-well sample, as expected from theory. The maximum shift $\Delta E_{11h} \simeq -20$ meV of the $11h$ transition was obtained for a field value of 45 kV/cm, above which the exciton becomes completely ionized. In addition, the linewidth (HWHM) of the $11h$ transition was observed to increase by approximately the same amount as the shift of the peak energy position, for a given electric field. Conclusively, the large Stark shift obtained in 250 Å wells is indicative of remarkable, exciton-related electro-optic properties, characterizing such a wide-well system at room temperature. However, the rather large field-induced linewidth broadening and the relatively low electric field at which the $11h$ exciton ionizes constitutes a drawback for the fabrication of efficient electro-optic devices, based on wide InGaAs/InAlAs QW systems.

ACKNOWLEDGMENT

This work was supported by the European Economics Communities program ESPRIT 3086 for Basic Research.

[1] C. Sirtori, F. Capasso, D. L. Sivco, S. N. G. Chu, and A. Y. Cho, Appl. Phys. Lett. **59**, 2302 (1991).
[2] Y. Le Bellego, J. P. Praseuth, and A. Scavennec, Electron. Lett. **27**, 2228 (1991).
[3] I. Kotaka, K. Wakita, K. Kawano, M. Asai, and M. Naganuma, Electron. Lett. **27**, 2162 (1991).
[4] D. A. B. Miller, D. S. Chemla, T. C. Damen, A. C. Gossard, and W. Wiegmann, Appl. Phys. Lett. **45**, 13 (1984).
[5] D. A. B. Miller, D. S. Chemla, T. C. Damen, A. C. Gossard, W. Wiegmann, T. H. Wood, and C. A. Burrus, Phys. Rev. Lett. **53**, 2173 (1984).
[6] K. Yamanaka, T. Fukunaga, T. Tsukada, K. L. I. Kobayashi, and M. Ishii, Appl. Phys. Lett. **48**, 840 (1986).
[7] P. W. Yu, G. D. Sanders, K. R. Evans, D. C. Reynolds, K. K. Bajaj, C. E. Stutz, and R. L. Jones, Appl. Phys. Lett. **54**, 2230 (1989).
[8] I. J. Fritz, T. M. Brennan, J. R. Wendt, and D. S. Ginley, Appl. Phys. Lett. **57**, 1245 (1990).
[9] R. P. Leavitt, J. W. Little, and S. C. Horst, Phys. Rev. B **40**, 4183 (1989).
[10] S. Nojima, Y. Kawamura, K. Wakita, and O. Mikami, J. Appl. Phys. **64**, 2795 (1988).
[11] K. Satzke, G. Weiser, W. Stolz, and K. Ploog, Phys. Rev. B **43**, 2263 (1991).
[12] A. S. Brown, U. K. Mishra, J. A. Henige, and M. J. Delaney, J. Appl. Phys. **64**, 3476 (1988).
[13] D. F. Welch, G. W. Wicks, and L. F. Eastman, Appl. Phys. Lett. **46**, 991 (1985).
[14] S. Hong and J. Singh, J. Appl. Phys. **62**, 1994 (1987).
[15] A. Dimoulas, J. Leng, K. P. Giapis, A. Georgakilas, C. Michelakis, and A. Christou, Phys. Rev. B (to be published)
[16] D. A. B. Miller, D. S. Chemla, T. C. Damen, A. C. Gossard, W. Wiegmann, T. H. Wood, and C. A. Burrus, Phys. Rev. B **32**, 1043 (1985).
[17] M. Matsuura and T. Kamizato, Phys. Rev. B **33**, 8385 (1986).
[18] B. V. Shanabrook, O. J. Glembocki, and W. T. Beard, Phys. Rev. B **35**, 2540 (1987).
[19] Y. S. Huang, H. Qiang, F. H. Pollak, J. Lee, and B. Elman, J. Appl. Phys. **70**, 3808 (1991).
[20] Y. Toyozawa, Prog. Theor. Phys. **20**, 53 (1958).
[21] M. A. Herman, D. Bimberg, and J. Christen, J. Appl. Phys. **70**, R1 (1991).
[22] G. K. Wertheim, M. A. Butler, K. W. West, and D. N. E. Buchanan, Rev. Sci. Instrum. **45**, 1369 (1974).
[23] W. M. Theis, G. D. Sanders, C. E. Leak, K. K. Bajaj, and H. Morkoc, Phys. Rev. B **37**, 3042 (1988).
[24] S. T. H. Abidi and S. N. Mohammad, J. Appl. Phys. **56**, 3341 (1984).
[25] G. Halkias, A. Georgakilas, J. L. Mourrain, and A. Christou, Solid-State Electron. **34**, 1157 (1991).
[26] G. Bastard, E. E. Mendez, L. L. Chang, and L. Esaki, Phys. Rev. B **28**, 3241 (1983).
[27] G. Bastard and J. A. Brum, IEEE J. Quantum Electron. **QE-22**, 1625 (1986).
[28] G. Bastard and R. Ferreira, Semicond. Sci. Technol. **5**, 470 (1990).